Thermal stability of biochar and its effects on cadmium sorption capacity

Fangjie Qi, Yubo Yan, Dane Lamb, Ravi Naidu, Nanthi S Bolan, Yanju Liu, Yong Sik Ok, Scott W. Donne, Kirk T Semple

PII: S0960-8524(17)31127-6
DOI: http://dx.doi.org/10.1016/j.biortech.2017.07.033
Reference: BITE 18453

To appear in: *Bioresource Technology*

Received Date: 30 May 2017
Revised Date: 5 July 2017
Accepted Date: 6 July 2017

Please cite this article as: Qi, F., Yan, Y., Lamb, D., Naidu, R., Bolan, N.S., Liu, Y., Ok, Y.S., Donne, S.W., Semple, K.T., Thermal stability of biochar and its effects on cadmium sorption capacity, *Bioresource Technology* (2017), doi: http://dx.doi.org/10.1016/j.biortech.2017.07.033

Thermal stability of biochar and its effects on cadmium sorption capacity

Fangjie Qi[1, 2], Yubo Yan[1, 3], Dane Lamb[1, 2], Ravi Naidu*[1, 2], Nanthi S Bolan[1, 2], Yanju Liu[1, 2], Yong Sik Ok[4], Scott W. Donne[5], Kirk T Semple[6]

[1]Global Centre for Environmental Remediation, ATC Building, Faculty of Science, The University of Newcastle, University Drive, Callaghan, NSW 2308, Australia

[2]Cooperative Research Centre for Contamination Assessment and Remediation of Environment (CRC CARE), The University of Newcastle, Callaghan NSW 2308, Australia

[3]Jiangsu Key Laboratory of Chemical Pollution Control and Resources Reuse, School of Environmental and Biological Engineering, Nanjing University of Science and Technology, Nanjing 210094, China

[4]Korea Biochar Research Center & School of Natural Resources and Environmental Science, Kangwon National University, Chuncheon 24341, Korea

[5]Discipline of Chemistry, University of Newcastle, Callaghan, NSW 2308, Australia

[6]Lancaster Environment Centre, Lancaster University LA1 4YQ, United Kingdom

*Corresponding author *E-mail* address: Ravi.Naidu@newcastle.edu.au

Abstract

In this study, the thermal stability of a wood shaving biochar (WS, 650 °C), a chicken litter biochar (CL, 550 °C) and an activated carbon (AC, 1100 °C) were evaluated by combustion at 375 °C for 24 h to remove the labile non-carbonized organic matter. Results showed that WS and CL biochars were not thermally stable and can lose most of the organic C during combustion. The combusted WS and CL biochars retained considerable amounts of negative charge and displayed higher sorption for Cd (from 5.46 to 68.9 mg/g for WS and from 48.5 to 60.9 mg/g for CL). The AC retained 76.5% of its original C and became more negatively chargely after combustion, but its sorption for Cd slightly decreased (from 18.5 to 14.9 mg/g). This study indicated that after potential burning in wildfires (200 - 500 °C), biochars could have higher sorption capacity for metals by remaining minerals.

Keywords: Biochar, stability, composition, cadmium, sorption

1. Introduction

Engineered pyrogenic carbon, biochars, are carbon-rich products produced through thermochemical processing of biomass under an oxygen-deficit environment (Venegas et al., 2015, Lehmann and Joseph, 2015). In the attempt to identify solutions to global environmental contamination issues, biochars from various sources have been widely reported to effectively sorb heavy metals in waste water and contaminated soils (Ahmad et al., 2014b, Qi et al., 2017b). For example, oak wood biochar was found to reduce the bioavailability of Pb in arms range soil (Ahmad et al., 2014a) and broiler litter biochar showed effectiveness in Cd, Cu, Ni, and Pb immobilization in water and soil (Uchimiya et al., 2010). Efficiency of metal removal from solution from different sources of biochars has also been demonstrated like dairy-manure biochar for Pb, Cd, Cu and Zn (Xu et al., 2013, Cao and Harris, 2010), municipal sludge biochar for Cd (Chen et al., 2014) and British broadleaf hardwood biochar for Pb, Ni, Cu and Zn (Shen et al., 2015).

Sorption properties of biochars for metals are dependent on their properties including composition and stability. All biochars contain organic carbonaceous phases (H, C, N, O, S) that are generally rich in surface functional groups and contribute largely to the high pH, negative charge, the cation exchange and surface complexation potential for metals (Mukherjee et al., 2011, Yuan et al., 2011). In addition to organic components, biochars also contain mineral components such as quartz, calcite, sylvite, periclase and whitlockite (Tsai et al., 2012, Cao and Harris, 2010). The mineral components of biochars can work as additional sorption sites for metals through electrostatic reaction and ion exchange (Xu and Chen, 2015, Zhao et al., 2015, Li et al., 2017), surface complexation (Qian and Chen, 2013, Zhang et al., 2013) and

formation of metal precipitates by releasing soluble ions like PO_4^{3-}, CO_3^{2-} and SO_4^{2-} (Inyang et al., 2012, Wang et al., 2015, Li et al., 2017).

When biomass is pyrolyzed in the aim of producing biochars, slow pyrolysis with moderate temperature (350-800 ˚C) is normally adopted (Qi et al., 2017b). Within this temperature range, most biochars are partially carbonized from biomass feedstocks. Therefore, the organic phase of biochars normally consists of carbonized organic matter that is more aromatic and more stable and non-carbonized organic matter that is relatively more aliphatic and less stable (Joseph et al., 2010, Chen et al., 2008). Biochar labile organic carbon phase can be easily oxidized during the biotic and abiotic ageing processes while the oxidation of more aromatic phase takes place more slowly (Mukome et al., 2014). Hence, the stability of biochars can influence their compoistion and thereby the sorption capacity.

Combustion activities can occur in the environment during wildfires (vegetation buring) and prescribed burnings (for agriculture and forest management), introducing charcoal (a type of natural biochar) into soils (Qi et al., 2017b). Given the widespread occurrences of the natural combustion processes (Qi et al., 2017b), both naturally produced and purposely amended biochars may be subjected to secondary combustion in the field. During this combustion process, the thermal stability of biochars can determine the compositional transformation and thereby the change of soprtion behaviours for contaminants.

In this study, a thermal oxidation method involving combusting biochars at 375 °C for 24 h was adopted to simulate the natural combustion (wildfires) processes (200 - 500 °C) (Raison, 1979). This method has been used to get rid of the non-pyrogenic organic matter of soils in order to measure soil pyrogenic carbon (stable

aromatic organic carbon) (Agarwal and Bucheli, 2011, Qi et al., 2017c). In this way, the proportion of the non-carbonized organic matter fraction and, therefore, the (thermal) stability of biochar organic phase can be evaulated. The subsequent changes of elemental composition, surface charge and sorption behaviours of biochars before and after thermal treatment were investigated. Cadmium (Cd) was selected as the model heavy metal due to its wide presence in agricultural soils caused by phosphate fertilizer application (Qi et al., 2017a).

2. Materials and Methods

2.1 Biochar treatment

In this study, a wood shaving (WS, 650 °C) biochar, a chicken litter (CL, 550 °C) biochar and one activated carbon were obtained commercially. The biochars were made by 16-minute slow pyrolysis (8 minutes in the drier, 8 minutes in the pyrolysis chamber) in a continuous flow pyrolyzer. Biochar products were water mist quenched immediately after pyrolysis, then additional water was hosed onto the bulk product. After purchase, biochars were ground to pass through a 2-mm sieve and dried before use. The activated carbon (AC, made from coal, steam activated 1100 °C) was a fine powder and subjected to no further grinding. The biochars and AC were then combusted in a porcelain plate at 375 °C for 24 h in a muffle furnace with air. Finally the original chars (WS, CL and AC) and combusted residues (denoted CLC, WSC and ACC, respectively) were ground and sieved to <150 μm prior to further study.

2.2 Characterization of biochars and AC

2.2.1 Chemical analysis

The pH and electrical conductivity (EC) of the 6 (original and treated) biochars and AC samples were determined using 1 : 20 solid to water ratio after shaking for

24h. The acid neutralization capacity (ANC) of biochar and AC samples was defined as the quantity of acid or base (cmol kg^{-1}) required to shift the initial pH of the material to a pH of 4 (Venegas et al., 2015) in a 1 : 300 solid : water ratio. Extractable cations and anions of the 6 samples were extracted by shaking 0.1 g of samples in 20 mL Milli-Q H_2O for 24 h before metal and anion analysis using inductively coupled plasma mass spectrometry (ICP-MS, Agilent 7900, USA) and ion chromatography (Metrohm 790 Personal IC, Switzerland), respectively. The contents (wt%) of carbon (C), hydrogen (H), nitrogen (N), sulphur (S) of biochars and AC were measured by a CHNS analyzer (Vario Micro cube, Elementar, Germany). Ash content (%) was measured by heating samples under 800 °C for 4 h in a muffle furnace. The weight percent (wt%) of oxygen (O) was determined by mass difference (Chen et al., 2008).

2.2.2 Surface charge properties

Zeta (electrokinetic) potential represents the net charge between the surface plane and slip plane of a colloidal particle (Zhao et al., 2015). The magnitude of its electro-negativity reflects the value of surface negative charges (Zhao et al., 2015). In this study, the surface charge characteristics of biochars and AC before and after combustion (< 150 μm) were estimated from their zeta potential values in aqueous suspension (0.02%, w/v) at pH values ranging from 3 to 10. Zeta potential was measured on Zetasizer Nano-ZS (Malvern ZEN3600, United Kingdom).

2.3 Batch sorption experiment for cadmium

2.3.1 Sorption methods

Cadmium (Cd) sorption was studied using a batch-type sorption experiments by agitating 0.2 g of sample in 40 ml of 0.01 M $NaNO_3$ solution containing 0, 0.5, 1, 2, 3, 5 mM $Cd(NO_3)_2$ on a reciprocating shaker at 200 rpm for 24 h (25 °C). After

sorption, the suspensions were centrifuged at 3500 rpm for 30 minutes and filtered through 0.22 µm syringe filter after pH measurement. The filtrates were separated into a few portions for different measurement. One portion was diluted and acidified immediately with 1 M HNO_3 prior to determination of Cd, Na, K, Ca, Mg, Fe, Al and Mn concentrations by ICP-MS (Agilent 7900, USA). Another portion was measured for major anions ($PO4^{3-}$, Cl^-, NO_3^-, SO_4^{3-}) by ion chromatography (Metrohm 790 Personal IC, Switzerland). From another portion, the total dissolved organic carbon (DOC) was analyzed by a total organic carbon analyzer (Multi N/C 3100, Analytik Jena, Germany). The amount of Cd sorbed was calculated from the difference between initial and final solution concentration. The analytical data, pH, DOC, anions, and cations at the initial Cd concentration of 2 mM were used to simulate Cd species by Visual MINTEQ 3.0. The effect of Cd on surface charge characteristics of biochar and AC samples was also investigated by comparing zeta potential of suspensions with 0 mM and 2 mM $Cd(NO_3)_2$. The biochar and AC residues after sorption under 0 mM and 4 mM $Cd(NO_3)_2$ were collected, washed with Milli-Q water and vacuum dried for post-sorption characterization. Fourier Transformed Infrared Spectroscopy (FTIR, Nicolet IS10, Thermo Fisher, Waltham, MA, USA) spectra were collected to get information on surface functional groups of biochar and AC samples. This was done by applying the dehydrated KBr disc technique, where biochar and AC samples (<150 µm) were mixed with spectroscopic grade KBr at a ratio of 1:50 before scanning to produce sufficient absorbance. Spectra over the 4000-400 cm^{-1} range were obtained by inclusion of 64 scans with a resolution of 4 cm^{-1} and a mirror velocity of 0.6329 cm/s. The X-ray diffraction (XRD) patterns of biochar and AC samples were derived using a Philips X'Pert MRD X-ray diffractometer with 45 position sample changer/spinner,

Cu anode tube and Pixcel 1d detector (The Netherlands) at the EMXRAY unit at the University of Newcastle. The mineral phases were identified by the X'Pert HighScore Plus software using the International Centre for Diffraction Data (ICDD) database.

Sorption kinetics was studied by shaking 2mM $Cd(NO_3)_2$ with biochar and AC samples for 10, 30, 60, 120, 240, 420, 630 and 1380 min on a reciprocating shaker at 200 rpm for 24 h at 25 °C. At the end of each equilibrium time, the mixtures were centrifuged and filtered through 0.22 μm syringe filters followed by dilution, acidification and detection of Cd by ICP-MS (Agilent 7900, USA). All sorption was conducted in duplicate with background solutions without sorbents used as controls. All results were expressed as an average of two replicates.

2.3.2 Sorption models

To evaluate and compare the sorption capacities and sorption features of Cd by different biochars, a few well-studied isotherm and kinetic models were employed to fit the sorption data.

Langmuir and Freundlich models were employed to describe the sorption isotherms. The linear forms of the two models are shown in Eq. (1) and (2) (Yan et al., 2015, Foo and Hameed, 2010):

$$\text{Langmuir model: } \frac{C_e}{q_e} = \frac{Ce}{q_{max}} + \frac{1}{bq_{max}} \quad (1)$$

$$\text{Freundlich model: } \log q_e = \log K_F + \frac{1}{n}\log C_e \quad (2)$$

where C_e (mg/L) and q_e (mg/g) are the equilibrium concentrations of Cd in solution and on sorbent samples, respectively. Langmuir constants q_{max} (mg/g) and b (L/g) represent maximum sorption capacity and sorption strength, respectively. The parameters K_F and n are Freundlich parameters related to the sorption capacity and sorption intensity, respectively.

To further understand the sorption types and mechanisms, Dubinin-Radushkevich (D-R) isotherm model (Eq. (3)-(5)) was applied to fit the sorption data (Yan et al., 2015, Foo and Hameed, 2010).

$$\ln q_e = \ln q_m - \beta\varepsilon^2 \qquad (3)$$

$$\varepsilon = RT\ln(1+\frac{1}{C_e}) \qquad (4)$$

$$E = \frac{1}{\sqrt{2\beta}} \qquad (5)$$

where q_e (mol/g) and C_e (mol/L) are the equilibrium Cd concentrations on sorbents and in solution, respectively, q_m (mg/g) is the theoretical saturation sorption capacity, β (mol^2/J^2) is a constant correlated with the mean free energy of adsorption, ε is the Polanyi potential, R (8.3145 J/mol/K) is the universal gas constant, T (K) is the absolute temperature in Kelvin, and E (J/mol) is the mean free energy of sorbing per molecule of sorbate from infinity in the solution to the surface of the solid.

The sorption kinetic data were fitted with the pseudo-first order (Eq. (6)) and pseudo-second order (Eq. (7)) kinetic models (Ho and McKay, 1999):

$$\log(q_t - q_e) = \log q_e - \frac{k_1 t}{2.303} \qquad (6)$$

$$\frac{t}{q_t} = \frac{1}{k_2 {q_e}^2} + \frac{t}{q_e} \qquad (7)$$

in which q_e (mg/g) and q_t (mg/g) are the amount of Cd sorbed at equilibrium and time t (min), k_1 (min^{-1}) and k_2 (g/mg/min) are the rate coefficient for pesudo-first order and pseudo-second order equation, respectively.

3. Results and Discussion

3.1 Stability and compositions of biochar and AC samples

Table 1 lists the properties of original and combusted biochar and AC samples. Combsution treatment resulted in a considerable decrease in total carbon (C) content of all original chars. The C content of the original CL biochar (33.7%) dropped to 0.68%

while that of WS biochar (75.6%) dropped to 33.8%. Since the inorganic carbon (ash) fractions of the two biochars were significantly increased, the reduced C content should be mainly from removal of the organic C phase. Hence, considering the biochar organic fraction consists of carbonized organic matter and non-carbonized organic matter, we defined carbonized organic matter as organic matter resisting combustion at 375 °C resembling non-pyrogenic organic matter of soils (Agarwal and Bucheli, 2011). The result from this study suggested the organic matter in our studied biochars was of low stability and mostly belonged to the labile non-carbonized organic matter fraction. This was implied by previous studies that char materials can be completely oxidized by the CTO-375 method (Brändli et al., 2009, Qi et al., 2017a) with no carbonized organic matter fraction observed. In contrast to biochars, AC, with a C content of 67.5% after combustion, could endure thermal treatment much better than biochars.

The ash content of WS, CL biochar and AC was 1.66%, 46.2% and 12.4%, respectively (Table 1). Following combustion, the corresponding ash content increased to 30.7%, 93.1% and 13.3% for WS, CL biochar and AC, respectively (Table 1). The supporting information contains the major water extractable mineral element levels of the 6 biochar and AC samples. The wood based WS biochar was found to be rich in Mg, Al, Ca, Fe, the manure based CL biochar was rich in Mg, K, Ca, P, while AC rich in Mg, Al, Ca, S. After thermal treatment, concentrations of biochar mineral elements largely increased due to the mineral phase enrichment. However, some elements like Ca and Mg in CL biochar and Al in AC declined after combustion. This was likely due to formation of new insoluble phases during combustion.

The studied original CL biochar (7.69) and AC (8.65) were of alkaline nature while WS biochar (4.20) was strongly acidic (Table 1). The CL biochar had a significantly higher acid neutralization capacity (ANC 222 cmol H^+/kg) compared to WS biochar (2.00 cmol H^+/kg) and AC (34 cmol H^+/kg). After combustion, both pH and ANC increased considerably for WS and CL biochars while that of AC dropped (Table 1). This increase in pH and ANC for WS and CL biochars were attributed to elevated levels of alkaline and alkaline earth elements (K, Ca, Na, Mg) (Mukome et al., 2013, Yuan et al., 2011, Xu and Chen, 2014).

3.2 Electrokinetic charge

Figure 1 shows the measured zeta potential (ζ) values for biochar and AC samples as a function of solution pH. The zeta potential of all samples decreased consistently with increasing pH suggesting more net negative surface charge at higher pH. Zeta potential of the two original biochar samples was negative within the entire pH range investigated (3-10). This was reflected in findings by Yuan and Xu (2011) who reported negative zeta potentials of all nine crop residue biochars within the pH range of pH 3-7 and in that by Xu and Chen (2014) who noted that zeta potentials for a series of rice bran biochars made at 300 or 700 °C were all negative within pH 3-10. After combustion at 375 °C, both WS and CL biochars became less negatively charged while AC became more negatively charged. Combusted CL biochar (CLC) was still negatively charged within the pH range of 3-10. Combusted WS biochar (WSC) became positively charged when the pH was below 5.5. These results suggest that the mineral fractions of biochars contribute considerably to the negative charge, which echoed the finding of Zhao et al., (2013, 2015) that mineral components in biochars can contribute to the cation exchange capacity (negative charge). Meanwhile,

the reduction of zeta potential after non-pyrogenic organic matter removal of both biochars confirmed the contribution of the biochar organic phase to the negative charge. Hence, our findings are consistent with previous studies in that biochar surface charge was determined by both the organic components and the mineral fractions (e.g., calcite, albite and silicate) (Qian and Chen, 2014, Zhao et al., 2015, Xu and Chen, 2014).

3.3 Sorption properties

3.3.1 Sorption isotherms

Soluble heavy metal(loid)s of biochars and AC in water extract were negligible (supporting information). Cadmium sorption isotherms by each of the biochars and AC samples are shown in Fig. 2. According to the isotherm classification by Limousin et al. (2007), CL biochars showed L type sorption where biochar surfaces progressively became saturated by Cd and the ratio of solution phase Cd to solid phase Cd decreased with increasing Cd loading. Combusted biochars WSC and CLC showed an H-type sorption, which is a particular form of L-type sorption with a high initial sorption affinity that the initial slope of the sorption isotherm approaches infinity. Samples WS, AC and ACC had linear C type sorption isotherms, which indicated the ratio of Cd concentration in solutions and on solid phases did not change with initial Cd concentration.

The Cd sorption isotherms of char samples matched Freundlich (R^2 = 0.86-0.98) and Langmuir model well (R^2 = 0.81-0.99), except the WS biochar (R^2 = 0.06) did not follow the Langmuir model (Langmuir q_{max} of WS biochar was still used for comparison). Calculated parameters from the two isotherm models are listed in Table

2. The Langmuir parameter q_{max} is the monolayer adsorption capacity. Sorption capacities (q_{max}) of WSC (68.9 mg/g), CL (48.5 mg/g) and CLC (60.9 mg/g) were much higher than that of AC (18.5 mg/g), ACC (14.9 mg/g) and WS (5.46 mg/g). Sorption capacity indicated by Freundlich constant K_F led to the same conclusion as that by q_{max}. After combustion, sorption capacity (q_{max}) of WS increased by 12.6 fold, that of CL increased by 1.26 fold while that of AC slightly decreased. The very low sorption of the original WS samples compared to WSC may be due to the strong acidity of WS biochar. The high sorption capacity of WSC suggested significant a sorptive role of mineral fractions of WS biochar which should have been facilitated by its alkaline nature. For CL biochar, removal of the organic fraction led to an increased sorption capacity, suggesting a more important role of the ash/mineral fraction of CL biochar on Cd sorption than the organic fraction. As for AC, the slight reduction in sorption capacity may be caused by decreased pH (from 8.65 to 4.76) and decreased organic C phase (Table 1).

Sorption strength b from the Langmuir model and n from Freundlich sorption model are parameters that indicate whether sorption is favourable or not (Yan et al., 2015). The value of 1/n were between 0-1 for all char samples except WS biochar (>1) (Table 2), suggesting favourable sorption for Cd by all chars except WS biochar (Yan et al., 2015). Values of b and n suggested increased sorption affinity for WS and CL biochar and decreased sorption affinity of AC upon combustion.

3.3.2 Sorption Kinetics

The sorption kinetics of char samples are shown in Fig. 3. The results showed the sorption of Cd by WS was rapid and reached equilibrium within 10 min, and that of WSC took 120 min. CL biochar needed 630 min to reach sorption steady state

while its combusted counterpart CLC took only 240 min. Sorption of AC took 120 min to equilibrate while ACC was quicker and finished by 10 min. The limited sorption capacity of WS and ACC (Xu et al., 2014) and acidic conditions may have caused the rapid sorption process.

The results of model fitting showed that the sorption kinetics of the studied biochar and AC samples fitted well with the pseudo-second order model (R^2=0.99-1.00) (Fig 3, Table 3). Kinetic data for WS, CL and AC can also be fitted to the pseudo-first order equation (R^2=0.43, 0.72 and 0.39, respectively), but the fits were poor compared to the pseudo-second order model. According to Inyang et al. (2015), the pseudo second-order model can describe most sorption processes of biochars for metals within the whole equilibrating time range, while the pseudo first-order may only apply for the initial 20-30 min. The review of previous sorption studies by Tan et al. (2015) suggested that heavy metal removal processes by biochars followed pseudo-second-order kinetics in most cases. Hence, our study was consistent with previous findings. Complying with pseudo-second-order model suggested chemisorption was the rate-limiting step of the sorption processes of our studied chars (Yan et al., 2015, Inyang et al., 2015). This also implied that the fast sorption (10 min) of WS and ACC char could be dominated by physisorption without the rate-limiting step.

3.3.3 Sorption mechanisms

The major physicochemical properties of biochars including BET specific surface area (SAA), surface charge, elemental composition and surface functional groups can influence the sorption process for metals. Heavy metals can be bound to chars through (1) direct electrostatic interactions between cationic metal and negatively charged carbon surfaces, (2) ionic exchange between metal ions and

ionizable protons at the surface of acidic carbon, (3) specific binding of metals by surface ligands (functional groups) abundant on biochar surfaces including proton exchange with delocalized π electrons of basic aromatic carbon and coordination with d-electrons, and (4) forming precipitants with soluble mineral ions or OH^- (Inyang et al., 2015, Qi et al., 2017b).

In this study, the BET specific surface area of the studied biochars increased after combustion (Table 1), which may have contributed to the increased sorption capacity of WS and CL biochar. Sorption capacity (q_{max}) of the 6 studied samples for Cd did not correlate with their specific surface area (data not shown), indicating specific surface area was not the governing factor of Cd sorption in this study. This is indicated by the fact that AC, which has smaller specific surface area than their combusted counterpart (ACC), exhibited a higher sorption capacity.

The decrease of zeta potential after Cd loading (comparing 2 mM and 0 mM Cd sorption systems) suggested the occurrence of electrostatic interaction between Cd and negatively charged biochar and AC surfaces (Fig. 4) (Cui et al., 2016, Qian and Chen, 2014, Qian et al., 2013). The degree of zeta potential drop (Δ zeta = zeta of 0 mM Cd – zeta of 2 mM Cd) should reflect the amount of Cd sorbed through electrostatic interaction. The WS and CL biochar had higher Δ zeta values than WSC and CLC, indicating more contribution of electrostatic reaction to Cd sorption of biochars than their combusted counterparts. AC showed an opposite trend to WS and CL biochar regarding this. Overall, the contribution of electrostatic reaction to total Cd sorption (Δ zeta) was in proportion to total negative charge of each sorbent sample. However, the sorption capacity (q_{max}) did not follow the same trend as the total negative surface charge. Samples WS, CL and ACC had greater negative charge but

displayed smaller sorption capacity. This indicated electrostatic reaction was not the dominant process differentiating sorption capacity of the studied biochars and AC.

For active sorption sites occupied by alkaline and alkaline earth metal cations (Na^+, Mg^{2+}, Ca^{2+}, K^+), replacing these cations of biochar or AC samples is a common mechanism for heavy metal immobilization (Uchimiya et al., 2010, Cui et al., 2016). The cations release caused by Cd sorption (mmol/g, after subtracting the amount released in the 0 mM suspensions from that released in 0.5, 1, 2, 3 and 5 mM sorption system) were calculated (supporting information). The amount of Cd sorbed was found to show a significant linear correlation with some of the cations, indicating exchange of these exchangeable cations with Cd played a role in the sorption processes (Cui et al., 2016). Among them, Na and Mg exchange contributed to sorption of Cd by WS biochar (mainly organic phase), Ca and Mg for WSC (mineral phase), Mg, Ca and K for CL (organic and mineral) and ACC (organic and mineral), Ca, Mg, Na, K for CLC (mineral) and AC (organic and mineral). This finding suggested both organic and mineral phases of biochars and AC can sorb Cd through cation exchange.

Surface complexation by functional groups associated with biochar surfaces is another key sorption mechanism for heavy metals (Sun et al., 2014, Cui et al., 2016). We used FTIR (supporting information) to investigate the changes of functional groups of biochar and AC samples after Cd sorption. Sample WS, WSC, CL, CLC had a band at around 3450-3463 cm^{-1} assigned as phenolic hydroxyl (-OH) groups (Tsai et al., 2012), a band at 1590 - 1641 cm^{-1} assigned to aromatic ring C=C functional groups (Wang et al., 2011), a stretching at around 1436-1463 cm^{-1} that was aromatic carbonyl/carboxylic groups (-COO/C=O) (Guo and Chen, 2014, Yuan et al., 2011)

and a peak at 1085-1110 cm^{-1} which was attributed to aliphatic ether C-O stretching (Tsai et al., 2012, Yang and Jiang, 2014). Similarly, AC and ACC had -OH, C=C and C-O functional groups as evidenced by FTIR spectrums. After Cd loading, the peaks either shifted to a new position or became stronger/weaker (except no change of C=C in WSC) (supporting information), indicating surface complexation of Cd with these functional groups. Since Cd^{2+} prefers to form soft-soft acid-base bonds, complexation of Cd to carbonyl (C=O) (Harvey et al., 2011) and aromatic ring C=C (Uchimiya et al., 2010, Xu et al., 2013) may have involved cation-π bonding with delocalized π electrons of these surface functionalities (proton exchange). This confirmed both organic and mineral phase of biochars can provide surface complexation sites for Cd.

The pH drop of the sorption systems with increased Cd loading (Fig. 5) suggested proton release from proton exchange of Cd with dissociable proton sites (Uchimiya et al., 2010) or forming $Cd(OH)_2$ precipitates (Xu and Chen, 2014, Dong et al., 2014, Inyang et al., 2012) may have contributed to sorption of Cd in the studied biochars and AC. Considering $Cd(OH)_2$ precipitation can form when pH ranges from 8 to 9 (Zhao et al., 2016, Sun et al., 2014), formation of $Cd(OH)_2$ may be a possible sorption mechanism for WSC, CLC, AC given an initial solution pH of over 9. However, the release of protons (calculated from the difference of protons in Cd loaded and Cd-free systems, supporting information) was minimal, indicating a minimal role of $Cd(OH)_2$ precipitation or proton exchange in sorption of Cd. That may be one of the reasons of undetectable $Cd(OH)_2$ by XRD (data not shown) and Visual MINTEQ modelling. Meanwhile, XRD analysis and Visual MINTEQ simulation (data not shown) confirmed $CdCO_3$ precipitates in WSC, CLC and AC chars. Previous

studies also detected formation of $CdCO_3$ by XRD in biochar sorption systems (Cao et al., 2009, Trakal et al., 2016).

The good fits of sorption data by the Dubinin-Radushkevich (D-R) model (Table 2, R^2=0.77-0.99) can aid in the further exploration of the sorption types and sorption mechanisms of the studied biochar and AC samples. The sorption with E (mean free energy of sorption) value < 8 kJ/mol indicates weaker physio-sorption (Van der Walls interactions), sorption with E ranging within 8 - 16 kJ/mol is mainly through ion exchange and sorption process with E > 16 kJ/mol is governed by stronger chemisorption (Yan et al., 2015). However, there may be no absolute boundary of E value between different types of sorption and transition zones may exist. Hence, our results (Table 2) indicated Cd sorption by WS char (E=6.29 kJ/mol) was largely via physio-sorption, char ACC sorption for Cd (E=8.13 kJ/mol) may cover both physio-sorption and ion exchange but physio-sorption should be dominating. Sorption of CL (E=15.9 kJ/mol) and AC (E=13.7 kJ/mol) for Cd may be governed by chemisorption and ion exchange together, whereas chemisorption should have controlled the sorption of WSC (E=17.6 kJ/mol) and CLC (E=19.8 kJ/mol). The sorption strength indicated by the E value confirmed the increased sorption strength of WS and CL biochar and slightly decreased sorption strength of AC after combustion, consistent with that indicated by Langmuir and Freundlich models.

Regarding specific sorption mechanisms, electrostatic reaction should be the main form of physisorption, cation exchange should be ion exchange and surface complexation should be chemisorption. Hence, the dominant sorption mechanisms of WS biochar and combusted AC is likely to be electrostatic reaction, and the mineral and organic phase contaning CL biochar and AC were surface complexation and

cation exchange ($CdCO_3$ precipitation also existed for AC). The mineral dominated WSC and CLC samples may have sorbed Cd mainly by surface complexation and precipitation. This study indicates that the mineral phases of biochars can contribute to the sorption of heavy metals such as Cd through direct electrostatic retention, ion exchange, surface complexation as well as precipitation.

3.4 Environmental implications

This study simulated the changes of composition and sorption behaviours of biochars in the field after being subjected to potential combustion by fires. Results showed that after the combustion treatment (375 °C for 24 h), 2.29%, 50.0% and 74.3% (w/w, noted as recovery rate R) of the original WS, CL biochars and AC were retained. The Langmuir sorption capacity (q_{max}) (Table 2) of original and combusted biochar and AC samples were noted as q_{max0} and q_{max1}, respectively. The contribution of sorption capacity from combusted biochars and AC to their original counterparts (%) was calculated from $q_{max1}\times R/q_{max0}\times 100$. Results showed that after combustion, 28.9%, 62.9% and 60.2% of the sorption capacity was retained from the original WS, CL biochar and AC, respectively. Hence, the absolute sorption capacity of WS and CL biochars were reduced after removing the labile organic phase, but the sorption affinity and sorption strength increased as indicated by Langmuir, Freundlich and Dubinin-Radushkevich sorption models. This indicated that the sorption of combusted biochars could be more stable and long-lasting. However, combustion was not favourable for AC in terms of both sorption capacity and sorption strength.

The higher remaining sorption capacity (62.9%) of CL biochar was because of the higher remaining mineral content (93.1%) while AC (60.2%) was due to more C (76.6%) retained. Though sorption capacity was most notably increased for WS

during combustion, the remaining WSC only contributed 28.9% of the original sorption capacity of WS biochar due to a low recovery rate (2.29%). Hence, on one hand, higher stability of biochars/AC does enhance its capacity to retain its original sorption capacities for Cd after losing its labile organic phase by potential wildfire burning in the natural environment. On the other hand, for biochars, it is the mineral fraction accumulated during combustion that contributed to the higher remaining sorption capacity and sorption affinity for Cd. The importance of the mineral fraction of biochars for metal sorption was also emphasized previously (Xu and Chen, 2014, Zhao et al., 2015, Xu and Chen, 2015, Xu et al., 2014). Meanwhile, enhancing pH and ANC of the sorption matrix is another important reason for mineral/ash fractions contributing to sorption of Cd. This study implies that in some cases, organic fractions of biochar (like WS and AC) may play a minor role in the sorption of metals, especially at the acidic condition (WS biochar). Biochars rich in minerals (WSC, CL, CLC) tend to be alkaline and can have a high and strong sorption for metals. Though some biochars are easily burnt by fires in the natural environment, the remaining mineral rich fractions can still hold a considerable proportion of surface negative charges and dispalyed a higher and stronger sorption for Cd. However, since biochar sorption capacity will be reduced after combustion in the field, the replenishment of biochars may be needed based on the estimated reduction of sorption capacity. Overall, manure-based biochars made from moderate temperates can be the priority option for Cd retention in the natural environment, given the high sorption capacity both before and after combustion as well as moderate cost to produce.

4. Conclusions

Biochars produced from chicken litter (CL) and wood shavings (WS) at moderate temperature (550 - 650 °C) had very low thermal stability and contained mostly labile non-carbonized organic carbon (OC) and very small amounts of stable carbonized OC. Hence, these biochars can readily lose the OC phase in wildfires (200 -500 °C) in the field leaving mostly the mineral components. Though not thermally stable, biochars without labile organic phase demonstrated higher and stronger retention of Cd due to the mineral phase. Mineral phases of biochars can contribute to Cd sorption by electrostatic reaction, ion exchange, surface complexation and precipitation.

(E-supplementary data for this work can be found in e-version of this paper online)

Acknowledgement

We acknowledge the Electron Microscope & X-Ray Unit of University of Newcastle, Australia for XRD analysis, Activated Carbon Technologies Pty Ltd (Australia) for providing activated carbon, Naser Khan for providing biochars, the Cooperative Research Centre for Contamination Assessment and Remediation of the Environment (CRC CARE) for financial support.

References

1. Agarwal, T., Bucheli, T.D. 2011. Is black carbon a better predictor of polycyclic aromatic hydrocarbon distribution in soils than total organic carbon? Environ. Pollut. 159, 64-70.

2. Ahmad, M., Lee, S.S., Lim, J.E., Lee, S.-E., Cho, J.S., Moon, D.H., Hashimoto, Y., Ok, Y.S. 2014a. Speciation and phytoavailability of lead and antimony in a small arms

range soil amended with mussel shell, cow bone and biochar: EXAFS spectroscopy and chemical extractions. Chemosphere. 95, 433-441.

3. Ahmad, M., Rajapaksha, A.U., Lim, J.E., Zhang, M., Bolan, N., Mohan, D., Vithanage, M., Lee, S.S., Ok, Y.S. 2014b. Biochar as a sorbent for contaminant management in soil and water: a review. Chemosphere. 99, 19-33.

4. Brändli, R.C., Bergsli, A., Ghosh, U., Hartnik, T., Breedveld, G.D., Cornelissen, G. 2009. Quantification of activated carbon contents in soils and sediments using chemothermal and wet oxidation methods. Environ Pollut. 157, 3465-3470.

5. Cao, X., Harris, W. 2010. Properties of dairy-manure-derived biochar pertinent to its potential use in remediation. Bioresour. technol. 101, 5222-5228.

6. Cao, X., Ma, L., Gao, B., Harris, W. 2009. Dairy-Manure Derived Biochar Effectively Sorbs Lead and Atrazine. Environ. Sci. Technol. 43, 3285-3291.

7. Chen, Zhou, D., Zhu, L. 2008. Transitional Adsorption and Partition of Nonpolar and Polar Aromatic Contaminants by Biochars of Pine Needles with Different Pyrolytic Temperatures. Environ. Sci. Technol. 42, 5137-5143.

8. Chen, T., Zhang, Y.X., Wang, H.T., Lu, W.J., Zhou, Z.Y., Zhang, Y.C., Ren, L.L. 2014. Influence of pyrolysis temperature on characteristics and heavy metal adsorptive performance of biochar derived from municipal sewage sludge. Bioresour. Technol. 164, 47-54.

9. Cui, X., Hao, H., Zhang, C., He, Z., Yang, X. 2016. Capacity and mechanisms of ammonium and cadmium sorption on different wetland-plant derived biochars. Sci. Total Environ. 539, 566-575.

10. Dong, X., Wang, C., Li, H., Wu, M., Liao, S., Zhang, D., Pan, B. 2014. The sorption of heavy metals on thermally treated sediments with high organic matter content. Bioresour. Technol. 160, 123-128.

11. Foo, K., Hameed, B. 2010. Insights into the modeling of adsorption isotherm systems. Chem. Eng. J.156, 2-10.

12. Guo, J., Chen, B. 2014. Insights on the Molecular Mechanism for the Recalcitrance of Biochars: Interactive Effects of Carbon and Silicon Components. Environ. Sci. Technol. 48, 9103-9112.

13. Harvey, O.R., Herbert, B.E., Rhue, R.D., Kuo, L.-J. 2011. Metal Interactions at the Biochar-Water Interface: Energetics and Structure-Sorption Relationships Elucidated by Flow Adsorption Microcalorimetry. Environ. Sci. Technol. 45, 5550-5556.

14. Ho, Y.S., McKay, G. 1999. Pseudo-second order model for sorption processes. Process Biochem. 34, 451-465.

15. Inyang, M., Gao, B., Yao, Y., Xue, Y., Zimmerman, A.R., Pullammanappallil, P., Cao, X. 2012. Removal of heavy metals from aqueous solution by biochars derived from anaerobically digested biomass. Bioresour. Technol. 110, 50-56.

16. Inyang, M.I., Gao, B., Yao, Y., Xue, Y., Zimmerman, A., Mosa, A., Pullammanappallil, P., Ok, Y.S., Cao, X. 2015. A review of biochar as a low-cost adsorbent for aqueous heavy metal removal. Crit. Rev. Environ. Sci. Technol. 0, 1-28.

17. Joseph, S.D., Camps-Arbestain, M., Lin, Y., Munroe, P., Chia, C.H., Hook, J., van Zwieten, L., Kimber, S., Cowie, A., Singh, B.P., Lehmann, J., Foidl, N., Smernik, R.J., Amonette, J.E. 2010. An investigation into the reactions of biochar in soil. Soil Res. 48, 501-515.

18. Lehmann, J., Joseph, S. 2015. Biochar for environmental management: science, technology and implementation. Routledge.

19. Li, H., Dong, X., da Silva, E.B., de Oliveira, L.M., Chen, Y., Ma, L.Q. 2017. Mechanisms of metal sorption by biochars: Biochar characteristics and modifications. Chemosphere. 178, 466-478.

20. Limousin, G., Gaudet, J.P., Charlet, L., Szenknect, S., Barthès, V., Krimissa, M. 2007. Sorption isotherms: A review on physical bases, modeling and measurement. Appl. Geochem. 22, 249-275.

21. Mukherjee, A., Zimmerman, A.R., Harris, W. 2011. Surface chemistry variations among a series of laboratory-produced biochars. Geoderma. 163, 247-255.

22. Mukome, F.N.D., Zhang, X., Silva, L.C.R., Six, J., Parikh, S.J. 2013. Use of Chemical and Physical Characteristics To Investigate Trends in Biochar Feedstocks. J. Agric. Food Chem. 61, 2196-2204.

23. Mukome, F.N.D., Kilcoyne, A.L.D., Parikh, S.J. 2014. Alteration of biochar carbon chemistry during soil incubations: SR-FTIR and NEXAFS investigation. Soil Sci. Soc. Am. J. 78, 1632-1640.

24. Qi, F., Dong, Z., Lamb, D., Naidu, R., Bolan, N.S., Ok, Y.S., Liu, C., Khan, N., Johir, M.A.H., Semple, K.T. 2017a. Effects of acidic and neutral biochars on properties and cadmium retention of soils. Chemosphere. 180, 564-573.

25. Qi, F., Kuppusamy, S., Naidu, R., Bolan, N.S., Ok, Y.S., Lamb, D., Li, Y., Yu, L., Semple, K.T., Wang, H. 2017b. Pyrogenic Carbon and Its Role in Contaminant Immobilization in Soils. Crit. Rev. Environ. Sci. Technol. Accepted.

26. Qi, F., Naidu, R., Bolan, N.S., Dong, Z., Yan, Y., Lamb, D., Bucheli, T.D., Choppala, G., Duan, L., Semple, K.T. 2017c. Pyrogenic carbon in Australian soils. Sci. Total Environ. 586, 849-857.

27. Qian, L., Chen, B. 2013. Dual Role of Biochars as Adsorbents for Aluminum: The Effects of Oxygen-Containing Organic Components and the Scattering of Silicate Particles. Environ. Sci. Technol. 47, 8759-8768.

28. Qian, L., Chen, B. 2014. Interactions of Aluminum with Biochars and Oxidized Biochars: Implications for the Biochar Aging Process. J. Agric. Food Chem. 62, 373-380.

29. Qian, L., Chen, B., Hu, D. 2013. Effective Alleviation of Aluminum Phytotoxicity by Manure-Derived Biochar. Environ. Sci. Technol. 47, 2737-2745.

30. Raison, R.J. 1979. Modification of the soil environment by vegetation fires, with particular reference to nitrogen transformations: A review. Plant Soil. 51, 73-108.

31. Shen, Z.T., Jin, F., Wang, F., McMillan, O., Al-Tabbaa, A. 2015. Sorption of lead by Salisbury biochar produced from British broadleaf hardwood. Bioresour. Technol. 193, 553-556.

32. Sun, J., Lian, F., Liu, Z., Zhu, L., Song, Z. 2014. Biochars derived from various crop straws: Characterization and Cd(II) removal potential. Ecotoxicol. Environ. Saf. 106, 226-231.

33. Tan, X., Liu, Y., Zeng, G., Wang, X., Hu, X., Gu, Y., Yang, Z. 2015. Application of biochar for the removal of pollutants from aqueous solutions. Chemosphere. 125, 70-85.

34. Trakal, L., Veselská, V., Šafařík, I., Vítková, M., Číhalová, S., Komárek, M. 2016. Lead and cadmium sorption mechanisms on magnetically modified biochars. Bioresour. Technol. 203, 318-324.

35. Tsai, W.-T., Liu, S.-C., Chen, H.-R., Chang, Y.-M., Tsai, Y.-L. 2012. Textural and chemical properties of swine-manure-derived biochar pertinent to its potential use as a soil amendment. Chemosphere. 89, 198-203.

36. Uchimiya, M., Lima, I.M., Thomas Klasson, K., Chang, S., Wartelle, L.H., Rodgers, J.E. 2010. Immobilization of Heavy Metal Ions (CuII, CdII, NiII, and PbII) by Broiler Litter-Derived Biochars in Water and Soil. J. Agric. Food Chem. 58, 5538-5544.

37. Venegas, A., Rigol, A., Vidal, M. 2015. Viability of organic wastes and biochars as amendments for the remediation of heavy metal-contaminated soils. Chemosphere. 119, 190-198.

38. Wang, X.S., Miao, H.H., He, W., Shen, H.L. 2011. Competitive Adsorption of Pb(II), Cu(II), and Cd(II) Ions on Wheat-Residue Derived Black Carbon. J. Chem. Eng. Data. 56, 444-449.

39. Wang, Z., Liu, G., Zheng, H., Li, F., Ngo, H.H., Guo, W., Liu, C., Chen, L., Xing, B. 2015. Investigating the mechanisms of biochar's removal of lead from solution. Bioresour. Technol. 177, 308-317.

40. Xu, X., Cao, X., Zhao, L., Wang, H., Yu, H., Gao, B. 2013. Removal of Cu, Zn, and Cd from aqueous solutions by the dairy manure-derived biochar. Environ. Sci. Pollut. Res. 20, 358-368.

41. Xu, X., Cao, X., Zhao, L., Zhou, H., Luo, Q. 2014. Interaction of organic and inorganic fractions of biochar with Pb(ii) ion: Further elucidation of mechanisms for Pb(ii) removal by biochar. RSC Adv. 4, 44930-44937.

42. Xu, Y., Chen, B. 2015. Organic carbon and inorganic silicon speciation in rice-bran-derived biochars affect its capacity to adsorb cadmium in solution. J. Soils Sediments. 15, 60-70.

43. Yan, Y., Li, Q., Sun, X., Ren, Z., He, F., Wang, Y., Wang, L. 2015. Recycling flue gas desulphurization (FGD) gypsum for removal of Pb(II) and Cd(II) from wastewater. J. Colloid Interface Sci. 457, 86-95.

44. Yang, G.-X., Jiang, H. 2014. Amino modification of biochar for enhanced adsorption of copper ions from synthetic wastewater. Water Res. 48, 396-405.

45. Yuan, J.-H., Xu, R.-K., Zhang, H. 2011. The forms of alkalis in the biochar produced from crop residues at different temperatures. Bioresour. Technol. 102, 3488-3497.

46. Yuan, J.H., Xu, R.K. 2011. The amelioration effects of low temperature biochar generated from nine crop residues on an acidic Ultisol. Soil Use Manage. 27, 110-115.

47. Zhang, P., Sun, H., Yu, L., Sun, T. 2013. Adsorption and catalytic hydrolysis of carbaryl and atrazine on pig manure-derived biochars: Impact of structural properties of biochars. J. Hazard. Mater. 244–245, 217-224.

48. Zhao, B., Xu, R., Ma, F., Li, Y., Wang, L. 2016. Effects of biochars derived from chicken manure and rape straw on speciation and phytoavailability of Cd to maize in artificially contaminated loess soil. J. Environ. Manage. 184, 569-574.

49. Zhao, L., Cao, X., Wang, Q., Yang, F., Xu, S. 2013. Mineral constituents profile of biochar derived from diversified waste biomasses: Implications for agricultural applications. J. Environ. Qual. 42, 545-552.

50. Zhao, L., Cao, X., Zheng, W., Wang, Q., Yang, F. 2015. Endogenous minerals have influences on surface electrochemistry and ion exchange properties of biochar. Chemosphere. 136, 133-139.

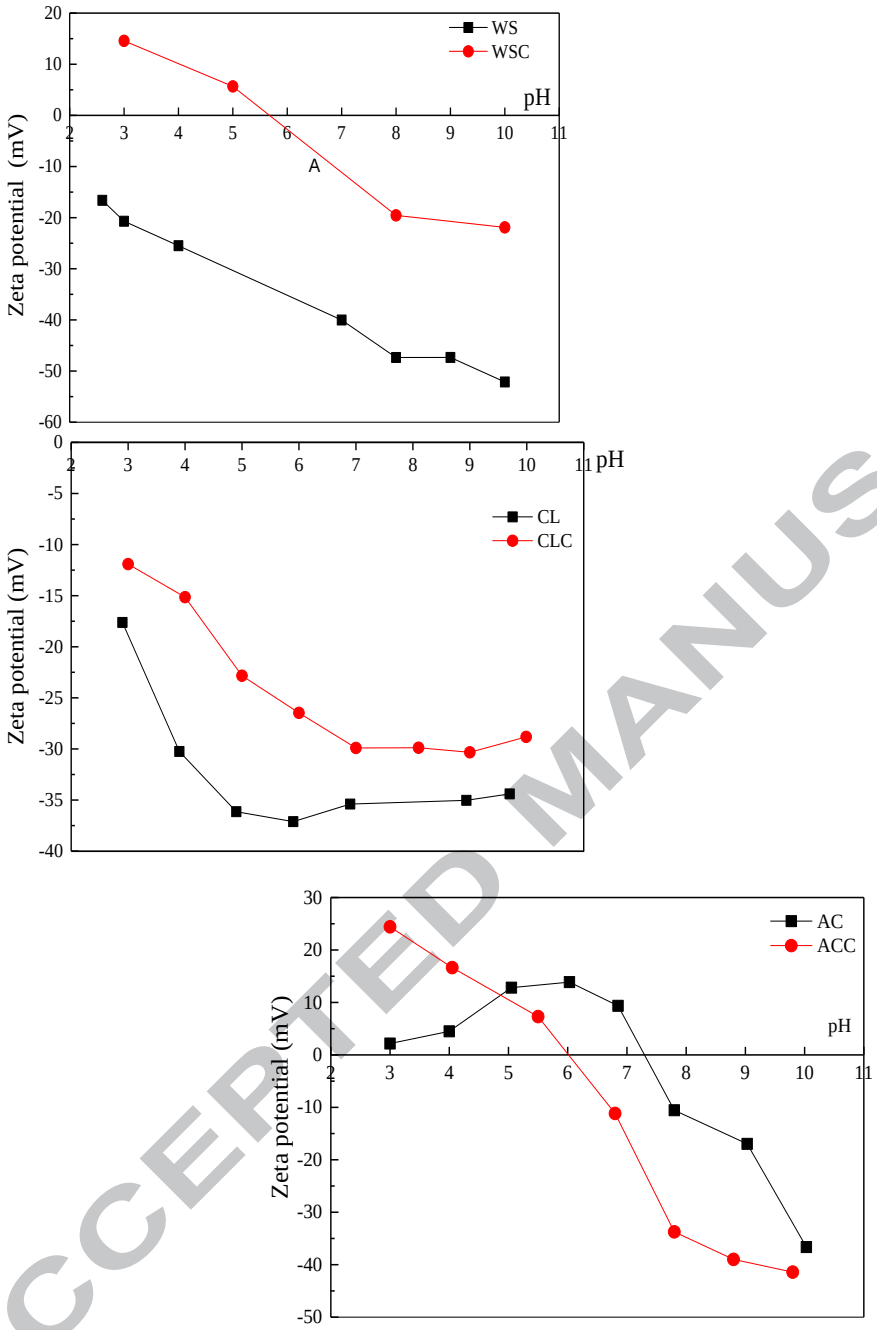

Fig 1. Zeta potential of biochar and activated carbon samples

Notes: WS, CL, AC- Wood shaving biochar, chicken litterbiochar and activated carbon, respectively; CLC, WSC, ACC- Combusted wood shavingbiochar, combusted chicken litter biochar and combusted activated carbon, respectively.

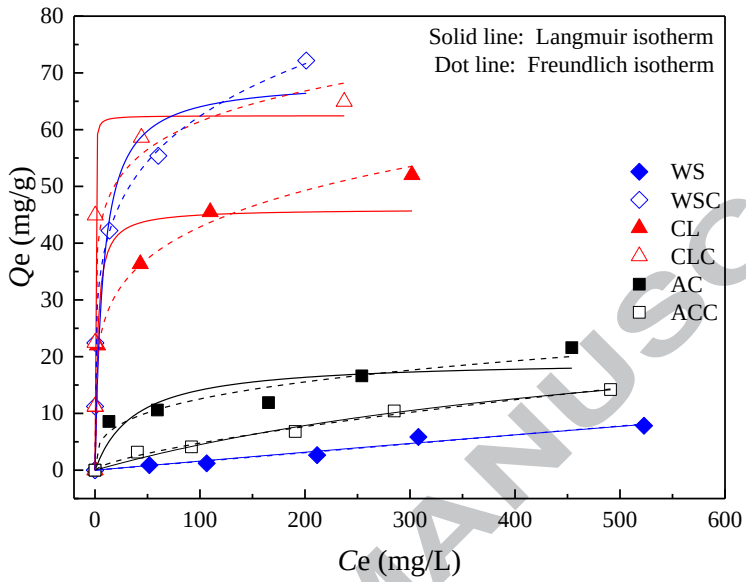

Fig 2. Sorption isotherms of biochar and activated carbon samples

Notes: WS, CL, AC- Wood shaving biochar, chicken litterbiochar and activated carbon, respectively; CLC, WSC, ACC- Combusted wood shavingbiochar, combusted chicken litter biochar and combusted activated carbon, respectively.

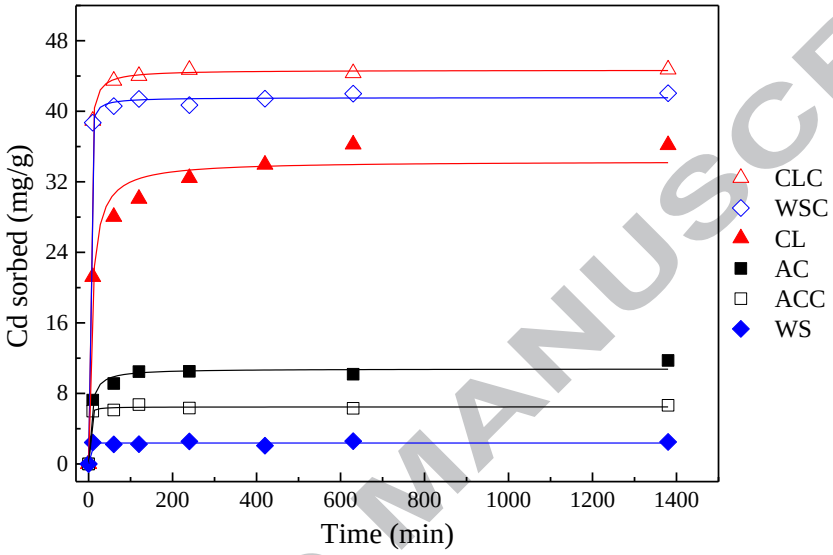

Fig 3. Sorption kinetics of biochar and activated carbon samples

Notes: WS, CL, AC- Wood shaving biochar, chicken litterbiochar and activated carbon, respectively; CLC, WSC, ACC- Combusted wood shavingbiochar, combusted chicken litter biochar and combusted activated carbon, respectively.

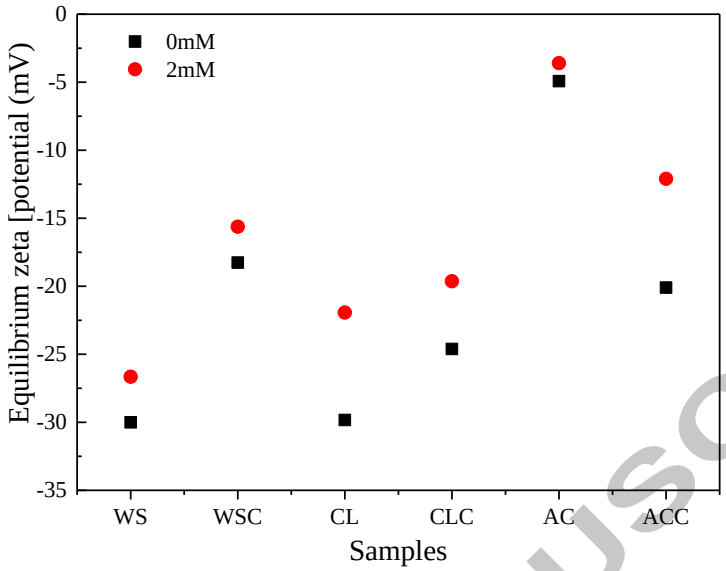

Fig 4. Zeta potential of biochars and AC in Cd loading and Cd free systems

Notes: WS, CL, AC- Wood shaving biochar, chicken litter biochar and activated carbon, respectively; CLC, WSC, ACC- Combusted wood shaving biochar, combusted chicken litter biochar and combusted activated carbon, respectively.

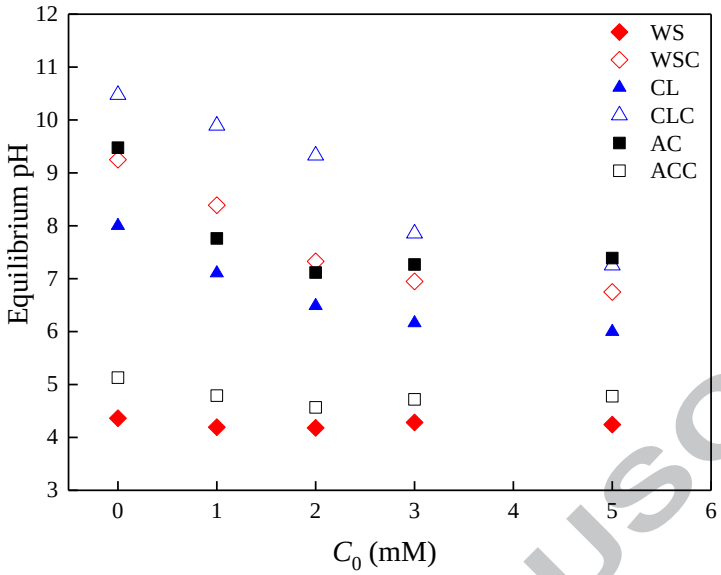

Fig 5. Equilibrium pH of Cd sorption systems by biochars and activated carbon

Notes: WS, CL, AC- Wood shaving biochar, chicken litterbiochar and activated carbon, respectively; CLC, WSC, ACC- Combusted wood shavingbiochar, combusted chicken litter biochar and combusted activated carbon, respectively.

Table 1. Characteristics of biochar and AC samples

Samples	C (%)	H (%)	N (%)	S (%)	O (%)	Ash (%)	[b]SSA (m^2/g)	pH[a]	EC[a] (dS/m)	[c]ANC (cmol H+/kg)
WS	75.6	3.23	0.25	0.32	18.9	1.66	1.05	4.20	67.3	2.00
WSC	33.8	1.42	0.49	0.36	18.2	30.7	248	9.07	809	215
CL	33.7	2.41	3.81	0.40	13.5	46.2	6.97	7.69	1450	222
CLC	0.68	0.60	0.08	0.83	4.78	93.1	16.4	10.6	2770	464
AC	79.5	0.67	0.34	0.55	6.56	12.4	863	8.65	72.4	34.0
ACC	60.8	1.60	0.24	0.41	23.7	13.3	1020	4.76	245	10.0

Notes: [a]EC, pH were measured with 1g sample : 20 mL H_2O; [b]SAA-specific surface area (BET); [c]ANC- acid neutralization capacity; WS, CL, AC- Wood shaving biochar, chicken litter biochar and activated carbon, respectively; CLC, WSC, ACC- Combusted wood shaving biochar, combusted chicken litter biochar and combusted activated carbon, respectively.

Table 2. Parameters of sorption isotherm models for biochars and AC

	Langmuir			Freundlich			D-R model		
Samples	q_{max} (mg/g)	b (L/mg)	R^2	1/n	K_F	R^2	q_m (mg/g)	E (kJ/mol)	R^2
WS	5.46	0.004	0.06	1.02	0.013	0.95	69.6	6.29	0.94
WSC	68.9	0.166	0.99	0.209	24.2	0.98	101	17.6	0.99
CL	48.5	0.134	0.99	0.224	15.5	0.97	80.8	15.9	0.99
CLC	60.9	1.09	0.91	0.159	31.4	0.72	99.3	19.8	0.77
AC	18.5	0.019	0.91	0.245	4.16	0.86	29.6	13.7	0.82
ACC	14.9	0.004	0.81	0.628	0.277	0.98	51.2	8.13	0.95

Notes: WS, CL, AC- Wood shaving biochar, chicken litter biochar and activated carbon, respectively; CLC, WSC, ACC- Combusted wood shaving biochar, combusted chicken litter biochar and combusted activated carbon, respectively.

Table 3. Parameters of sorption kinetics models for biochars and AC

Pseudo-second order model			Pseudo-first order model
qe (mg/g)	K_1 (1/min)	R^2	R^2
2.51	0.71	0.99	0.43
42.0	0.000040	1.00	0.10
36.5	0.00034	0.99	0.72
44.6	0.000020	1.00	0.01
11.6	0.013	0.99	0.39
6.62	0.020	0.99	0.07

Notes: WS, CL, AC- Wood shaving biochar, chicken litter biochar and activated carbon, respectively; CLC, WSC, ACC- Combusted wood shaving biochar, combusted chicken litter biochar and combusted activated carbon, respectively.

Highlights

- Moderate temperature (550-650°C) biochars contained mostly labile organic C (OC).
- Biochar OC was not thermally stable and easily oxidized by wildfire (200 -500 °C).
- Combusted (375°C) biochars were mineral dominant and negatively charged.
- Biochar combustion residues showed a higher and stronger sorption capacity for Cd.

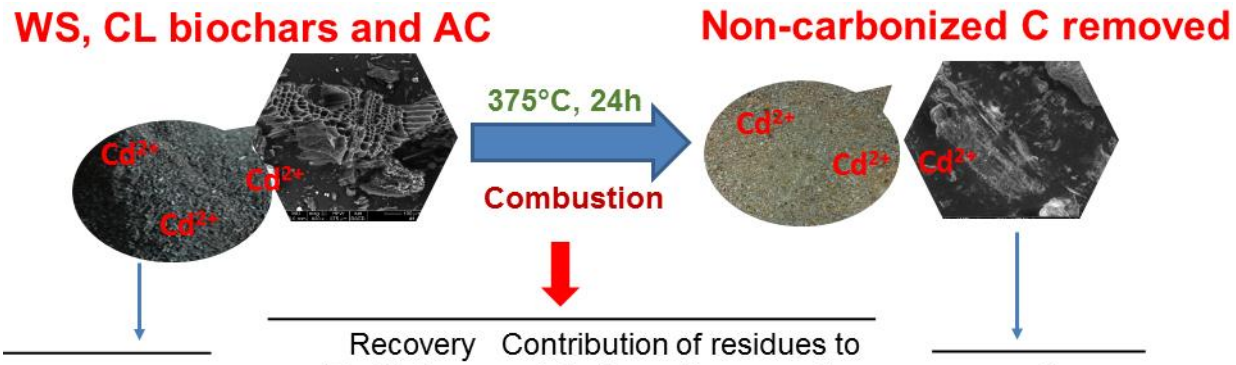

	q_{max0} (mg/g)
WS	5.46
CL	48.5
AC	18.5

	Recovery (R, %) from combustion	Contribution of residues to original sorption capacity (%, $=q_{max1}/q_{max0}*R*100$)
WS	2.29	28.9
CL	50.0	62.6
AC	74.3	60.2

	q_{max1} (mg/g)
WSC	68.9
CLC	60.9
ACC	14.9